

Adaptive filtering in EEG Signal for Artifacts Removal using Learning Algorithm

Quazi M. H

Swami Ramanand Theerth Marathwada University
Nanded, Maharashtra, India
quazimateenh@gmail.com

Dr. S. G. Kahalekar

Grahmin Polytechnic
Nanded, Maharashtra, India

Abstract: The brain's electrical activity and behavior is the neurophysiologic measurement by Electroencephalogram (EEG) by making a record of the EEG signal from the electrodes placed at the scalp. In most of the cases, the EEG signal gets muddle up with other biological signals and hence leads to artifacts. In the medical field, it is a challenging task to remove these artifacts from the EEG signal. This paper formulates a novel artifact removal model from multi-channel EEG data by hybridizing the Grey Wolf Optimization (GWO) and FireFly (FF) algorithm. Initially, the optimal weights of the EEG signal are achieved by feeding the input EEG signal to the proposed adaptive filtering. In the adaptive filtering technique, the clean EEG signal is recovered by means of subtracting the filtered output from the primary input. In the proposed adaptive filtering technique, the weights of NARX neural network need to be optimized to enhance the rejection accuracy. GWO and FF combine the weight of NARX neural network and hence optimize the weights. Finally, a performance-based evaluation is carried out between the proposed NN-GWO and FF and existing ICA, WICA, FICA, NN-GWO, and NN-FF in terms of MSE and RMSE with different artifacts like ECG, EMG and EOG.

Keywords: EEG Signal; NARX Neural Network; Adaptive Noise Cancelation; NN-GWO+FF approach

1. Introduction

The most significant information resource so far not heavily untouched for activity recognition of the brain signal is EEG [6][7]. The spontaneous electrical activity of the brain signals from the scalp is recorded by EEG over a small interval of time. In the nervous system, the language of communication between the neurons is electric and the information in the neurons is processed by means of changing the flow of electrical currents. This change in the direction of the flow of electrical currents generates electric and magnetic fields and they are recorded from the surface of the scalp by placing electrodes [8] [9]. In the scalp, the brain signals originate from the post-synaptic potentials, aggregates at the cortex, and transfers through the skull to the scalp. The electrical activity of the brain is recorded by the potential difference between the electrodes. In recent times, there has been noteworthy development in the brain signal recoding techniques [10] [15]. Moreover, with the aid of the signal processing techniques, the EEG data from the brain are extracted using Bayesian Inference and these signals gets converted into device control commands. In EEG, the recording of the cerebral activities of the brain is accomplished with the help of the electrodes, which are attached to the surface of the skull. Then, the feature extraction of the recorded EEG signals from the electrodes undergoes amplification, filtration, and digitalization for processing of the recorded signal in the computer [11] [12]. Then, from the feature extracted signals, the classification of the signals, as well as the control command, is generated. This is a key technology for paralyzed patients, who suffer from severe neuromuscular disorders [13] [16]. These EEG recordings for eye movement tracking are non-invasive and low cost. Apart from this, it suffers from a deep challenge of pattern recognition as well as signal processing and defected signals.

The amplitude of the EEG signal is small and hence they become more contaminated by noise. The signal recorded by EEG is not always in the pure form and it has some defected signals like power line noise, electrode noise, eye movement, muscle contraction and these defects (noise) are referred as artifacts [17] [18]. Due to the availability of the artifacts signals in EEG recordings, it is a bit complex to extract the EEG signal accurately. electrode noise, baseline movement, Electromyography (EMG) disturbance are the few types of noise that accompany the EEG signal during recordings [14]. Hence, it is essential to remove this unwanted signal from the recorded EEG signal in order to extract the original

brain signal. Apart from this, it is more complex to remove the artifacts from the recorded EEG signal [19] [20].

In recent times, a vast count of techniques is available in EEG for removal of artifacts. Few techniques make use of ICA (independent component analysis), filtering as well as regression, WT (Wavelet Transform) and Adaptive Neuro-Fuzzy Inference System (ANFIS). The sorting of the recorded EEG signal obtained from the electrodes is accomplished by Independent Component Analysis (ICA) and this model failed in removing the artifacts during source separation [21] [22]. PCA technique rejected the artifacts signal and it was able to handle boisterous as well as concurrent data. This technique failed as it diminished the orthogonal rotation. The adaptive filter technique is another solution to the removal of the eye-blink artifacts and here the artifacts were removed by means of subtracting the EEG source signal from the estimated inference signal [23]. While compared to all other technique, the adaptive filters are efficient in real-time mode artifacts removal and the computation complexity of this model is low. Previously existing conventional algorithms [30] [31] [32] [33] [34] [35] have been used with different models to detect EEG peaks in various applications. Apart from these advantages, it suffers from the drawback that the faults in the recorded signals weren't eliminated [24] [25].

The major contribution of this research work is to present the EEG signal and the artifact signal are fed initially as input to adaptive filtering and the clean EEG signal is retrieved. In the NARX neural network model, three types of weights are combined using the hybridized GWO+FF model. The weight of both the GWO and FF is optimized in the NARX neural network by adaptive filtering. The performance of the proposed GWO+FF model is compared with the existing models like ICA, WICA, FICA, NN-GWO, NN-FF in terms of MSE and RMSE with different artifacts like ECG, EMG, and EOG.

The rest of the paper is organized as follows: Section 2 describes the literature review, and Section 3 defines the architecture of the proposed adaptive noise cancellation for Artifacts removal. Section 4 describes the Proposed training Algorithm for NARX Neural Network model. Section 5 summarizes the result and discussion and section 6 concludes the paper.

2. Literature Review

In 2014, Julie et al. [1] have investigated the sleep subjects that were attained directly from EEG with an unsupervised learning scheme and topic representation. In addition, these approaches have deployed PSG data for evolving with this scheme. Also, the implemented technique was deployed to PolySomnoGram (PSG) data. Simultaneously, the data was separated into 2 datasets such as validation and training datasets. In addition, a characteristic denoting EEG features depending on topics was also evaluated. Feature subsets were further approximated by means of Lasso-regularized regression scheme.

In 2017, Quazi et al.[2]formulated a novel Deep Learning Network (DLN) with two stages viz. offline stage and online stage for removing the artifacts in the recorded EEG signal. In the offline stage, the high-order statistical moment's information was gathered by means of cutting off the ocular artifacts in the samples used to train DLN. In the online stage, the trained DLN were filtered in an automatic way by removing the ocular artifacts. The proposed model was compared with the existing modeling classic ICA, Second-Order Blind Identification (SOBI) and kurtosis-ICA (K-ICA) with the data collected from a public database and lab individual data. The resultant of the analysis exhibited higher generalization ability in the proposed model.

In 2019, Dora et al.[3]proposed Variational Mode Decomposition (VMD) as an enhanced version of signal decomposition scheme to suppress ocular artifacts from the recorded EEG signal. The Multiscale Modified Sample Entropy (mMSE) was utilized to identify the ocular artifact corrupted segment. The count of the Band-Limited Intrinsic Mode Functions (BLIMFs) and the balancing parameter helped in identifying BLIMFs, low-frequency BLIMFs as well as high amplitude BLIMFs. The Empirical Mode Decomposition (EMD) and ICA were employed to remove the artifacts in the signal.

In2016, Zou, et al.[4]projected an innovative algorithm with two major phases for identifying and removing artifact in the recorded EEG signal. The artifacts that had the physiological origins were identified using an event-related feature-based clustering algorithm. The nonbiological artifacts were identified with the help of the electrode-scalp impedance information. The resultant of the proposed model exhibited improvement in signal quality and had removed both physiological and nonbiological artifacts

In 2017, Garg et al.[5]developed a novel technique with adaptive filtering for removal of ocular artifacts of EEG. Here, the Horizontal EOG (HEOG) and Vertical EOG (VEOG) signals were recorded separately as two reference inputs and these signals were processed using the Finite Impulse Response (FIR) filters. The Numerical Variable Forgetting Factor (NVFF), as well as the recursive least squares (RLS) algorithm, were utilized for the adaptively updating of linear filter coefficients. Further, the artifact-free EEG signal was acquired by subtracting the processed HEOG and VEOG signals.

3 Architecture of the proposed Adaptive Noise Cancellation for Artifacts Removal

The artifacts from the EEG signal are generally removed with the help of the adaptive noise cancellation. The main intention of this technique is to recover the clean EEG signal [28]. The block diagram of the adaptive noise cancellation is illustrated in Fig.1. Initially, the adaptive noise cancellation process requires two inputs, one from the EEG signal source and the other from the source of the artifact signal. The input generated from the EEG signal source and the artifact source signal is represented as $S_i(t)$ and $A_i(t)$, respectively. The source of noise here is the origin in which different types of artifacts are generated. The interference signal is generated, when the artifacts noise source passes via the unidentified non-linear dynamics. The interference signal is depicted using the term $I_i(t)$. Then, the primary input signal is generated by combining both the interference signal $I_i(t)$ and the clean source signal $S_i(t)$. The mathematical formula for the primary input signal $P_i(t)$ is expressed in Eq. (1). The filtered output is achieved by a signal generated from the noise source $A_i(t)$ into the adaptive filtering process. The achieved filtered output $F_i(t)$ is similar to the interference signal generated from the nonlinear dynamics. Further, with the intention of retrieving the clean EEG signal, the achieved filtered output $F_i(t)$ is subtracted from the primary input signal $P_i(t)$. The mathematical formula for the adaptive noise cancellation in a clean EEG signal is depicted in Eq. (2).

$$P_i(t) = S_i(t) + I_i(t) \quad (1)$$

$$S_{i_o}(t) = S_i(t) + I_i(t) - F_i(t) \quad (2)$$

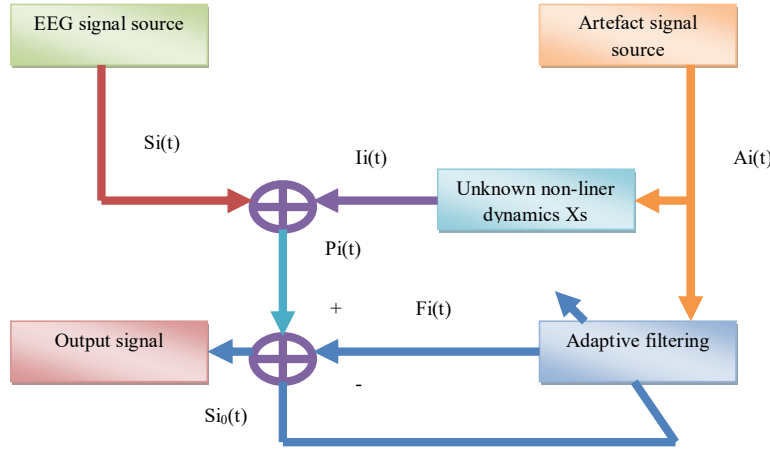


Fig. 1. Block diagram of adaptive noise cancellation

3.1 NARX System Model

The non-linear systems in this research work are modeled using the NARX neural network model [29]. The NARX neural network is the combination of multilayer feedforward network, recurrent loop and time delay. The NARX system model encloses the input layer, the hidden layers and the output layer within itself. The exogenous input vector and delayed exogenous input vector, as well as delayed regressed output vector, are available in the input layer. Apart from the non-linear systems modeling, the NARX neural network is also utilized for the analysis of the time series prediction. Typically, the time series prediction is based on the successively correlated signal that is related to the past values of the signal as well as the input signal. The output vector of NARX system model after performing the neural network operation is depicted using the term $Li(n+1)$. The mathematical formula for the output of NARX neural network model is shown in Eq. (3). The exogenous input vector is represented as $Li(n)$ and the terms $Li(n-1), Li(n-2), \dots, Li(n-Di_{Li})$ are the delay elements of the regressed output vector. The delayed exogenous input vector is represented using the term $Vi(n), Vi(n-1), \dots, Vi(n-Di_{Vi})$. In the initial stage, the weighting parameter is applied to the hidden units and the exogenous input vector as well as in between the hidden units and regressed output vector.

$$Li(n+1) = f(Li(n), \dots, Li(n-Di_{Li}), Vi(n-Di_{Vi})) \quad (3)$$

4. Proposed Training Algorithm for NARX Neural Network model

4.1 Standard GWO

GWO [27] is a new meta-heuristic algorithm introduced by Mirjalili and Lewis in the year 2014 on the basis of the inspiration gathered from leadership hierarchy and the hunting behavior of grey wolves. The top-level powers rest within α (alpha) grey wolves, which are in the apex of the hierarchy. The decisions on hunting are made by α . The one who assists α in the decision-making process is β (beta), who is next to α in the hierarchy. At the foot of the hierarchy lies ω (omega) that bows other wolves. In between β and ω lies the δ (delta) wolves. The upcoming section portrays the mathematical model of GWO.

Mathematical model of GWO

(i) **Search for prey (exploitation):** in this phase, α , β and δ generates unique solutions based on their searching process. The 1st, 2nd and 3rd best solutions are generated by α , β and δ , respectively and all other solutions are generated by ω .

(ii) **Encircling prey:** during the hunting process, the grey wolves encircle their prey. The mathematical equations corresponding to prey encircling behavior of grey wolves is shown in Eq. (4). The current iteration t , coefficient vectors, position vector T and S , position vector of the prey Xi_{prey} as well as the position vector of a grey wolf Xi are utilized in the prey encircling process in Eq. (5), Eq.(6). In addition, Eq. (6) and Eq. (7) random values in $[0, 1]$ are manifested as ra_1 and ra_2 . Here, the parameter b is varying from $[0, 2]$.

$$R = |S \cdot Xi_{prey}(t) - Xi(t)| \quad (4)$$

$$Xi(t+1) = Xi(t) - T \cdot R \quad (5)$$

$$T = 2 \cdot b \cdot ra_1 - b \quad (6)$$

$$S = 2 \cdot ra_2 \quad (7)$$

(ii) **Hunting the prey:** The location of prey and encircling of prey are major abilities of the grey wolf. α guides the hunting process and β and ω rarely participates in the hunting process. In the abstract search space there lacks no information on the location of the optimal prey. Such that, better knowledge of the potential location of the prey can be acquired from α , β and δ wolves. On the basis of the best search agent, the position of the prey is updated as per Eq. (8) to Eq. (17).

$$R_\alpha = |S_1 \cdot Xi_\alpha - Xi| \quad (8)$$

$$Xi_1 = Xi_\alpha - T_1 \cdot (R_\alpha) \quad (9)$$

$$R_\beta = |S_2 \cdot Xi_\beta - Xi| \quad (10)$$

$$Xi_2 = Xi_\beta - T_1 \cdot (R_\beta) \quad (11)$$

$$R_\delta = |S_3 \cdot Xi_\delta - Xi| \quad (12)$$

$$Xi_3 = Xi_\delta - T_1 \cdot (R_\delta) \quad (13)$$

$$Xi(t+1) = \frac{S_1 + S_2 + S_3}{3} \quad (14)$$

(iv) **Attacking the prey (exploitation):** once the prey is encircled it is attacked by the wolves and this hunting takes place only when the prey is stationary.

4.2 Standard Firefly Algorithm

FF algorithm [26] was introduced on the basis of the inspiration got from the fireflies by Xin-She Yang in 2008. In FF algorithms three main assumptions were made to evaluate the required optimal solution, (a) all FF are unisex (b) Attractiveness of FF are directly proportional to brightness and attractiveness of FF and it is inversely proportionally to distance between fireflies (c) The brightness of FF is defined in terms of objective function. Further, each of the fireflies has its own attractive function ρ and it is found to be indirectly proportional to the distance x . Further, the attractiveness in between two FF is depicted as per Eq. (15) the maximum attractiveness is indicated as ρ_0 and it is the light absorption coefficient. In addition, two FF are denoted as g and h and the position of these two FF are depicted as K_g and K_h , respectively. The distance between the FF is determined using the mathematical equation Eq. (16), where the count of the dimensions is indicated as b . The mathematical equation corresponding to the movement of FF is represented as per Eq. (17). Further, on the basis of the distance between FF, the

light intensity M_h of FF is predicted. The first term of the mathematical equation depicts the current position of FF, whereas the second term of the equation indicates the attractiveness of FF. The last term depicts the random movement of FF. The initial position of FF is denoted as per Eq. (18). The pseudo-code for conventional FF is shown in Algorithm 1. The mathematical equation of FF is shown in Eq. (18) in which M_0 represents the original light intensity.

$$M = M_0 e^{-\gamma x} \quad (15)$$

$$\rho(x) = \rho_0 e^{-\gamma x}, \quad v \geq 1 \quad (16)$$

$$x_{gh} = \|K_g - K_h\| = \sqrt{\sum_{w=1}^b (K_{g,w} - K_{h,w})^2} \quad (17)$$

$$K_{best} = K_g + \rho_0^{-\gamma x_{gh}^2} (K_h - K_g) + \omega \left(\text{rand} - \frac{1}{2} \right) \quad (18)$$

Algorithm 1: Firefly algorithm [26]

```

Initialize Maximum generation  $\text{Max}_g$  and intensity of light  $M_g$ 
Light absorption coefficient is defined
While ( $t < \text{Max}_g$ )
  For  $g = 1 : n_1$  for all FF
    For  $h = 1 : n_2$  for all FF
      If ( $M_h > M_g$ )
        FF  $g$  is moved towards  $h$ 
      End if
      Attractiveness varies with distance  $x$ 
      New solutions are evaluated and light intensity is updated
    End for  $h$ 
  End for  $g$ 
  FF are ranked and the best FF is predicted
End while

```

4.3 Objective Function and Solution Encoding

The foremost objective of this research is to optimize the weight of the neural network with the help of the hybrid FF+ GWO algorithm. The weight generated from GWO and FF is represented in Eq. (19) and Eq. (20). The weight vectors of both GWO and FF are hybridized using GWO+FF algorithm and the new weight vector generated is shown in Eq. (21).

$$wt^{GWO} = wt^{GWO1} + wt^{GWO2} + wt^{GWO3} + \dots + wt^{GWO_k} \quad (19)$$

$$wt^{FF} = wt^{FF1} + wt^{FF2} + wt^{FF3} + \dots + wt^{FF_k} \quad (20)$$

$$wt^{hb} = wt^{1(FF+GWO)} + wt^{2(FF+GWO)} + wt^{3(FF+GWO)} + \dots + wt^{k(FF+GWO)} \quad (21)$$

4.4 Proposed GWO+FF Algorithm for the NARX Model

The conventional GWO suffers from the drawbacks of bad local searching ability, low solving precision and slow convergence. So, the proposed GWO+FF are formulated. The architecture of the proposed GWO+FF algorithm for NARX neural network model is exhibited in Fig.3. The proposed GWO+FF model combines three kinds of weights and the weight input vector is formulated from the exogenous input weight, regressed output weight and the combination of both exogenous as well as the regressed output weights. The input for GWO and FF is the randomly generated input vector. Then, the optimization takes place and at the end of the optimizations processes, the weight vector of GWO and FF is generated. In the NARX neural network, the first training algorithm is the GWO algorithm and the operations of FF depend on the blinking characteristics. The position of FF gives the possible solution vector and on the basis of the brightness value, the position of FF is changed. In the absence of the brightness, FF makes random movement and hence the computation complexity increases. The conventional FF suffers from the drawback of lower convergence and leads to local optimal generation. To overcome the shortcoming of FF, faster convergence nonlinear optimization algorithm referred to as GWO is used along with FF. The GWO helps in finding the location of the object and helps in escaping from the problem of local optima. The conventional GWO suffers from the drawbacks of bad local searching ability, low solving precision and slow convergence. Thus, to overcome the drawbacks of both FF and GWO, they both are hybridized

to form GWO+FF. The proposed GWO+FF algorithm, when applied to NARX neural network, enhances the accuracy of artifacts removal. The architecture of the proposed GWO+FF algorithm for NARX neural network model is exhibited in Fig.2. The proposed GWO+FF model combines three kinds of weights and the weight input vector is formulated from the exogenous input weight, regressed output weight and the combination of both exogenous as well as the regressed output weights. The input for GWO and FF is the randomly generated input vector. Then, the optimization takes place and at the end of the optimizations processes, the weight vector of GWO and FF is generated.

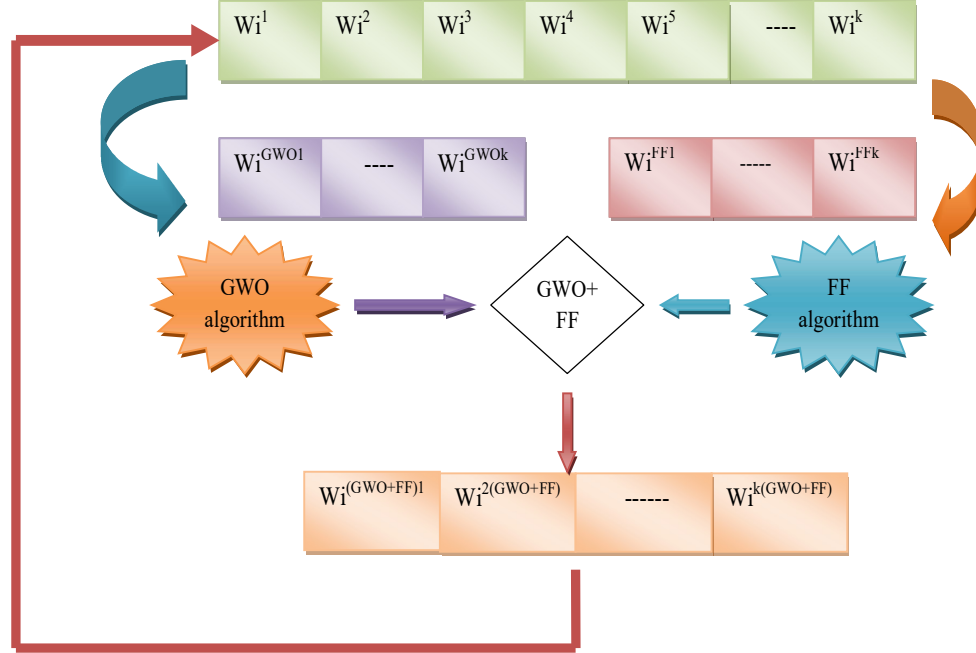


Fig. 2. Proposed hybrid learning algorithm (GWO+FF) for NARX Neural Network

5. Result and Discussion

The proposed artifact removal technique formulated by hybridizing GWO and FF is implemented in MATLAB with the real-time signals obtained from the physionet database. In order to exhibit the performance of the proposed NARX model, the real signal is contaminated with various artifacts signal sources such as EOG, EMG, and ECG. The input signals for EEG is obtained from https://physionet.org/cgi-bin/atm/ATM?database=ptbdb%26tool=plot_waveforms (access data: 2019-05-01). The ECG signal is obtained from https://physionet.org/physiobank/database/emgdb/emg_healthy.txt (access data: 2019-05-01) and EOG signal from https://physionet.org/cgi-bin/atm/ATM?database=ptbdb%26tool=plot_waveforms (access data: 2019-05-01). The physiologic signal is sampled at 256 samples per second with 16-bit resolution. The performance of the proposed model is compared with the existing models like ICA, WICA, FICA and NN-GWO in terms of Mean Square Error (MSE) and Root Mean Square Error (RMSE).

5.1 Performance Analysis based on MSE

Fig.3 illustrates the performance analysis of the proposed NN-GWO+FF model over the existing models in terms of MSE for various signals. In Fig. 3(a) for EEG signal with ECG artifact, the 1st signal is 71.4%, 73.3% and 86.6%, 88%, and 49% better than the existing models like ICA, WICA, and FICA, NN-FF and NN-GWO, respectively in terms of MSE. An enhancement of 76.4%, 75.9%, 75%, 85%, and 87% is recorded by the proposed NN-GWO+FF model over the existing models like ICA, WICA and FICA, NN-FF and NN-GWO, respectively in terms of MSE for 2nd signal relating to EEG signal with EMG artifact in Fig.3(b). Then, Fig.3(c) depicts the performance of the EEG signal with EOG artifact for 3rd signal and an improvement of 74.1%, 73.8%, 72%, 80%, and 85% is recorded by the proposed NN-GWO+FF model over the existing models like ICA, WICA and FICA, NN-FF and NN-GWO, respectively in terms of MSE.

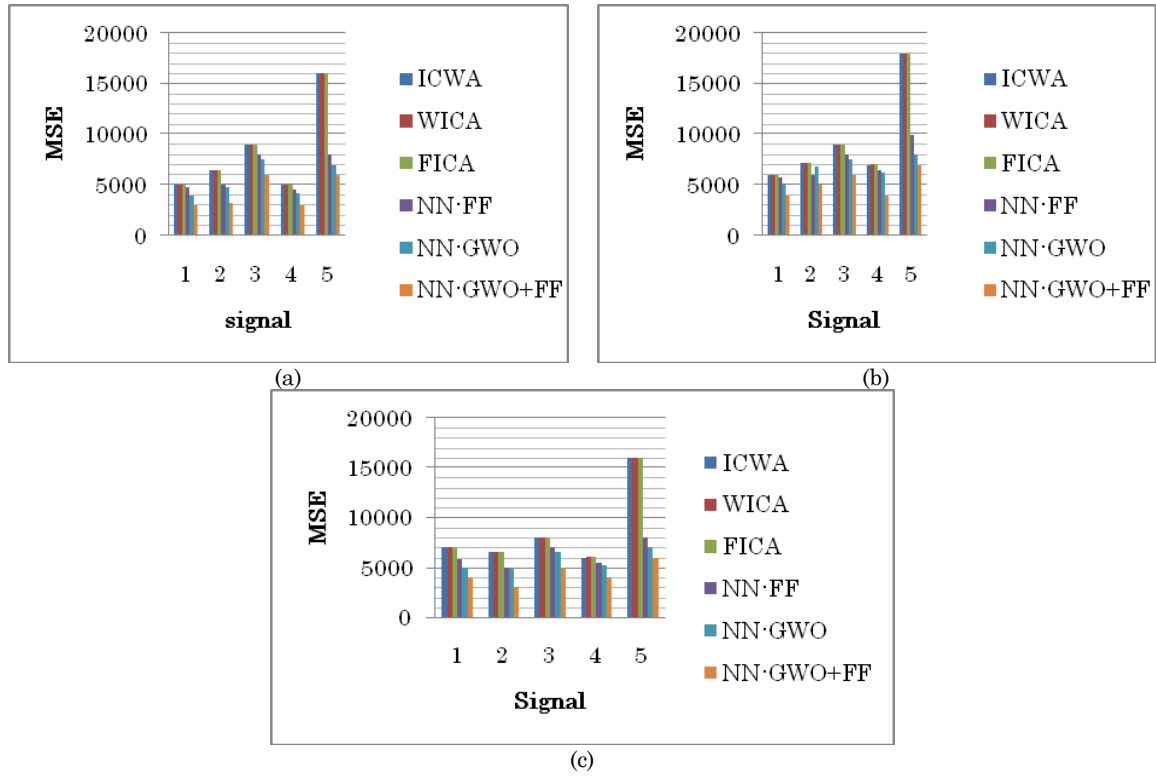


Fig. 3. MSE analysis of (a) EEG signal with ECG artifact (b) EEG signal with EMG artifact (c) EEG signal with EOG artifact

5.2 Performance Analysis Based on RMSE

Table 1 represents the performance analysis of the proposed NN-GWO+FF model over the existing models in terms of RMSE. For EEG signal with ECG artefact the performance of EEG signal with EOG artefact for 3rd signal and an improvement of 74.1%, 73.8%, 72%, 80% and 85% is recorded by the proposed NN-GWO+FF model over the existing models like ICA, WICA and FICA, NN-FF and NN-GWO, respectively in terms of RMSE, the proposed NN-GWO+FF model is 50% better than ICWA, 31.5% better than WICA, 28.5% better than FICA, 16.6% better than NN-FF and 7.6% better than NN-GWO. Table 2 depicts the performance analysis of the proposed NN-GWO+FF model over the existing models in terms of RMSE for EEG signal with EMG artifact. The proposed NN-GWO+FF model is 55.5%, 52.9%, 51.2 %, 42.8%, and 38.4% better than the traditional models like ICWA, WICA, FICA, NN-FF and NN-GWO, respectively in terms of RMSE. Further, RMSE of the EEG signal with EOG artifact is 66.6%, 64.2%, 62.9%, 33.3%, and 20% better than the state-of-art models like ICWA, WICA, FICA, NN-FF and NN-GWO, respectively in Table 3.

Table 1. RMSE analysis of EEG signal with ECG artefact

Signal	ICWA	WICA	FICA	NN-FF	NN-GWO	NN-GWO+FF
1	75	73	70	60	65	50
2	80	70	75	65	60	40
3	90	83	80	75	65	50
4	65	60	56	40	43	30
5	90	93	92	62	55	45

Table 2. RMSE analysis of EEG signal with EMG artefact

Signal	ICWA	WICA	FICA	NN-FF	NN-GWO	NN-GWO+FF
1	90	83	80	75	65	50
2	65	63	62	50	45	30
3	72	70	68	50	45	40
4	90	93	92	62	55	45
5	89	85	82	70	65	40

Table 3. RMSE analysis of EEG signal with EOG Artefact

	ICWA	WICA	FICA	NN-FF	NN-GWO	NN-GWO+FF
1	70	73	70	60	65	50
2	65	63	62	50	45	30
3	60	56	54	30	25	20
4	65	60	56	40	43	30
5	90	93	92	62	55	45

6. Conclusion

This paper focused on developing a hybrid optimization algorithm for artifact removal from the multi-channel EEG data. Initially, the EEG signal and the artifact signal were fed as input to the adaptive filtering in order to recover the clean EEG signal. The weights of the NARX neural network were found using the proposed hybrid optimization algorithm that hybridized the concept of GWO and FF. In the NARX neural network, the weight of both the GWO and FF was optimized by using the adaptive filtering. The performance of the proposed GWO+FF model was compared with the existing models like ICA, WICA, FICA, NN-GWO, NN-FF in terms of MSE and RMSE with different artifacts like ECG, EMG, and EOG. the performance of EEG signal with EOG artifact for 3rd signal and an improvement of 74.1%, 73.8%, 72%, 80%, and 85% are recorded by the proposed NN-GWO+FF model over the existing models like ICA, WICA and FICA, NN-FF and NN-GWO, respectively in terms of MSE. RMSE of the EEG signal with EOG artifact is 66.6%, 64.2%, 62.9%, 33.3%, and 20% better than the state-of-art models like ICWA, WICA, FICA, NN-FF and NN-GWO.

Compliance with Ethical Standards

Conflicts of interest: Authors declared that they have no conflict of interest.

Human participants: The conducted research follows the ethical standards and the authors ensured that they have not conducted any studies with human participants or animals.

References

- [1] Henriette Kocha, Julie A.E. Christensena, Rune Frandsenb, Marielle Zoetmuldere, Lars Arvastsonc, Soren R. Christensenc, Poul Jennumb, and Helge B.D. Sorensen, "Automatic sleep classification using a data-driven topic model reveals latent sleep states," *Journal of Neuroscience Methods*, vol. 235, pp. 130–137, September 2014.
- [2] M. H. Quazi, S. G. Kahalekar, "Artifacts removal from EEG signal: FLM optimization-based learning algorithm for neural network-enhanced adaptive filtering", *Biocybernetics and Biomedical Engineering*, vol.37, no.3, pp.401-411, 2017.
- [3] Chinmayee Dora, Pradyut Kumar Biswal, "An improved algorithm for efficient ocular artifact suppression from frontal EEG electrodes using VMD", *Biocybernetics and Biomedical Engineering*, In press, Available online April 2019.
- [4] Y. Zou, V. Nathan and R. Jafari, "Automatic Identification of Artifact-Related Independent Components for Artifact Removal in EEG Recordings," in *IEEE Journal of Biomedical and Health Informatics*, vol. 20, no. 1, pp. 73-81, Jan. 2016.
- [5] Harish Kumar Garg, Amit Kumar Kohli, "Excision of Ocular Artifacts from EEG Using NVFF-RLS Adaptive Algorithm", *Circuits, Systems, and Signal Processing*, vol.36, no.1, pp 404–419, 2017.
- [6] W. De Clercq, B. Vanrumste, J. -. Papy, W. Van Paesschen and S. Van Huffel, "Modeling common dynamics in multichannel signals with applications to artifact and background removal in EEG recordings," in *IEEE Transactions on Biomedical Engineering*, vol. 52, no. 12, pp. 2006-2015, Dec. 2005.
- [7] S. Khatun, R. Mahajan and B. I. Morshed, "Comparative Study of Wavelet-Based Unsupervised Ocular Artifact Removal Techniques for Single-Channel EEG Data," in *IEEE Journal of Translational Engineering in Health and Medicine*, vol. 4, pp. 1-8, 2016
- [8] K. Hermans et al., "Effectiveness of Reference Signal-Based Methods for Removal of EEG Artifacts Due to Subtle Movements During fMRI Scanning," in *IEEE Transactions on Biomedical Engineering*, vol. 63, no. 12, pp. 2638-2646, Dec. 2016.
- [9] R. Mahajan and B. I. Morshed, "Unsupervised Eye Blink Artifact Denoising of EEG Data with Modified Multiscale Sample Entropy, Kurtosis, and Wavelet-ICA," in *IEEE Journal of Biomedical and Health Informatics*, vol. 19, no. 1, pp. 158-165, Jan. 2015.
- [10] Y. Zou, V. Nathan and R. Jafari, "Automatic Identification of Artifact-Related Independent Components for Artifact Removal in EEG Recordings," in *IEEE Journal of Biomedical and Health Informatics*, vol. 20, no. 1, pp. 73-81, Jan. 2016.

- [11] M. Chavez, F. Grosselin, A. Bussalb, F. De Vico Fallani and X. Navarro-Sune, "Surrogate-Based Artifact Removal From Single-Channel EEG," in *IEEE Transactions on Neural Systems and Rehabilitation Engineering*, vol. 26, no. 3, pp. 540-550, March 2018.
- [12] S. R. Sreeja, R. R. Sahay, D. Samanta and P. Mitra, "Removal of Eye Blink Artifacts From EEG Signals Using Sparsity," in *IEEE Journal of Biomedical and Health Informatics*, vol. 22, no. 5, pp. 1362-1372, Sept. 2018.
- [13] G. Wang, C. Teng, K. Li, Z. Zhang and X. Yan, "The Removal of EOG Artifacts From EEG Signals Using Independent Component Analysis and Multivariate Empirical Mode Decomposition," in *IEEE Journal of Biomedical and Health Informatics*, vol. 20, no. 5, pp. 1301-1308, Sept. 2016.
- [14] S. Selvan and R. Srinivasan, "Removal of ocular artifacts from EEG using an efficient neural network based adaptive filtering technique," in *IEEE Signal Processing Letters*, vol. 6, no. 12, pp. 330-332, Dec. 1999.
- [15] M. M. N. Mannan, M. A. Kamran and M. Y. Jeong, "Identification and Removal of Physiological Artifacts From Electroencephalogram Signals: A Review," in *IEEE Access*, vol. 6, pp. 30630-30652, 2018.
- [16] M. M. N. Mannan, M. A. Kamran and M. Y. Jeong, "Identification and Removal of Physiological Artifacts From Electroencephalogram Signals: A Review," in *IEEE Access*, vol. 6, pp. 30630-30652, 2018.
- [17] C. Y. Sai, N. Mokhtar, H. Arof, P. Cumming and M. Iwahashi, "Automated Classification and Removal of EEG Artifacts With SVM and Wavelet-ICA," in *IEEE Journal of Biomedical and Health Informatics*, vol. 22, no. 3, pp. 664-670, May 2018.
- [18] K. Nazarpour, Y. Wongsawat, S. Sanei, J. A. Chambers and S. Orintara, "Removal of the Eye-Blink Artifacts From EEGs via STF-TS Modeling and Robust Minimum Variance Beamforming," in *IEEE Transactions on Biomedical Engineering*, vol. 55, no. 9, pp. 2221-2231, Sept. 2008.
- [19] Q. Zhao et al., "Automatic Identification and Removal of Ocular Artifacts in EEG—Improved Adaptive Predictor Filtering for Portable Applications," in *IEEE Transactions on NanoBioscience*, vol. 13, no. 2, pp. 109-117, June 2014.
- [20] L. Shoker, S. Sanei and J. Chambers, "Artifact removal from electroencephalograms using a hybrid BSS-SVM algorithm," in *IEEE Signal Processing Letters*, vol. 12, no. 10, pp. 721-724, Oct. 2005.
- [21] I. Daly, R. Scherer, M. Billinger and G. Müller-Putz, "FORCE: Fully Online and Automated Artifact Removal for Brain-Computer Interfacing," in *IEEE Transactions on Neural Systems and Rehabilitation Engineering*, vol. 23, no. 5, pp. 725-736, Sept. 2015.
- [22] A. Mahadevan, S. Acharya, D. B. Sheffer and D. H. Mugler, "Ballistocardiogram Artifact Removal in EEG-fMRI Signals Using Discrete Hermite Transforms," in *IEEE Journal of Selected Topics in Signal Processing*, vol. 2, no. 6, pp. 839-853, Dec. 2008.
- [23] P. LeVan, S. Zhang, B. Knowles, M. Zaitsev and J. Hennig, "EEG-fMRI Gradient Artifact Correction by Multiple Motion-Related Templates," in *IEEE Transactions on Biomedical Engineering*, vol. 63, no. 12, pp. 2647-2653, Dec. 2016.
- [24] X. Li, C. Guan, H. Zhang and K. K. Ang, "Discriminative Ocular Artifact Correction for Feature Learning in EEG Analysis," in *IEEE Transactions on Biomedical Engineering*, vol. 64, no. 8, pp. 1906-1913, Aug. 2017.
- [25] I. Daly, M. Billinger, R. Scherer and G. Müller-Putz, "On the Automated Removal of Artifacts Related to Head Movement From the EEG," in *IEEE Transactions on Neural Systems and Rehabilitation Engineering*, vol. 21, no. 3, pp. 427-434, May 2013.
- [26] IztokFister, IztokFisterJr, Xin-SheYang and JanezBrest, "A comprehensive review of firefly algorithms", *Swarm and Evolutionary Computation*, vol. 13, pp. 34-46, 2013.
- [27] Seyedali Mirjalili, Seyed Mohammad Mirjalili, Andrew Lewis, "Grey Wolf Optimizer", *Advances in Engineering Software*, Vol.69, pp. 46-61, 2014.
- [28] Jafarifarmand A, Badamchizadeh MA. Artifacts removal in EEG signal using a new neural network enhanced adaptive filter. *Neurocomputing*, vol. 103, pp.222–31,2013.
- [29] Menezes Jr JMP, Barreto GA. Long-term time series prediction with the NARX network: an empirical evaluation. *Neuro Computer*, vol.71:pp.3335–43,2008.
- [30] D. Menaga and Dr.S. Revathi,"Privacy Preserving using Bio Inspired Algorithms for Data Sanitization",International Conference on Electrical, Electronics, Computers, Communication, Mechanical and Computing (EECCMC); pp. 201-206, 2018.
- [31] MNKMSS Dr. N. Krishnamoorthy,"Performance Evaluation of Optimization Algorithm Using Scheduling Concept in Grid Environment", *The IIOAB Journal* 7 (9), pp. 315-323, 2016.
- [32] SB Vinay Kumar, PV Rao, Manoj Kumar Singh,"Multi-culture diversity based self adaptive particle swarm optimization for optimal floorplanning",*Multiagent and Grid Systems*, vol14, no.1, pp.31-65, 2018.
- [33] R Gupta Roy, D Baidya,"Speed Control of DC Motor Using Fuzzy-Based Intelligent Model Reference Adaptive Control Scheme",*Advances in Communication, Devices and Networking, Lecture Notes in Electrical Engineering* book series, Springer, vol. 462, pp.729-735, 2018.
- [34] G Singh, VK Jain, A Singh, "Adaptive network architecture and firefly algorithm for biogas heating model aided by photovoltaic thermal greenhouse system",*Energy & Environment*, vol. 29 (7), pp.1073-1097, 2018.
- [35] A Shankar, J Natarajan,"Base Station Positioning in Wireless Sensor Network to aid Cluster Head Selection Process", *International Journal of Intelligent Engineering and Systems*, vol. 10, no.(2), pp.173-182, 2017.